Eur. Phys. J. D **39**, 49–57 (2006)
DOI: 10.1140/epjd/e2006-00079-1

THE EUROPEAN PHYSICAL JOURNAL D

Modulational instability of dust acoustic waves in a dusty plasma with nonthermal electrons and ions

A.P. Misra[1,2] and A. Roy Chowdhury[2,a]

[1] Department of Mathematics, Siksha Bhabana, Visva-Bharati University Santiniketan-731 235, India
[2] High Energy Physics Division, Department of Physics, Jadavpur University Kolkata-700 032, India

Received 31 October 2005 / Received in final form 19 December 2005
Published online 11 April 2006 –

Abstract. Effects of nonadiabaticity of variable dust charge, dust fluid temperature, trapped electrons as well as nonisothermality of ions on the amplitude modulation of dust acoustic waves in an unmagnetized dusty plasma are investigated. A modified nonlinear Schrödinger equation (NLSE) is obtained by the standard reductive perturbation technique and is solved numerically by the split-step Fourier method. The modulational instability and the envelope solitary wave structure are found to be modified somewhat by the effects of nonthermally distributed ions and trapped electrons.

PACS. 52.35.Sb Solitons; BGK modes – 52.35.Mw Nonlinear phenomena: waves, wave propagation, and other interactions – 52.30.Ex Two-fluid and multi-fluid plasmas – 52.35.-g Waves, oscillations, and instabilities in plasmas and intense beams

1 Introduction

Theoretical as well as experimental investigations on modulational instability of ion-acoustic and dust acoustic waves in a dispersive and nonlinear plasma medium have been increasing because of their possible applications in space physics, astrophysics and also in many laboratory situations. By incorporating the effects of harmonic generation and ponderomotive nonlinearities, many authors have derived the nonlinear Schrödinger equation (NLSE) which governs the dynamics of the nonlinear modulated acoustic wave packet and the structure of the envelope solitary wave [1–10]. In the NLSE the nonlinearities are in great balance with the wave group dispersion. Theoretical investigations suggest that the presence of dust fluid temperature, nonadiabatic dust charge variation can affect the modulational instability of the dust acoustic wave [6].

When streaming particles be injected in a plasma, it has been found that instead of developing into a turbulent one, they evolve towards a coherent trapped particle state [11]. When an amplitude of a nonlinear wave becomes large, some electrons are trapped and carried out along with the wave. It is to be mentioned that the inclusion of trapped electrons or ions gives rise nonlinear phenomena of waves. However, it has been found that the electron and ion distributions play a significant role in characterizing the physics of nonlinear waves [12–15]. They offer considerable increase in richness and varieties of wave motions which can exist in plasmas. Also, the inclusion of thermal effects affects the nature of wave-particle interaction and possibility of having nonisothermal electron distribution in the potential well instead of the usual Boltzmannian. When the amplitude of the nonlinear wave becomes large, electrons are trapped in the potential trough, and as matter of fact the trapping of electrons is not a question of strength of the amplitude. The trapping of plasma particles which as a nonlinear process violates the linear wave ansatz is known from the early days of Plasma Physics [16] and is valid even for small amplitude limit, as proposed, probably for the first time by Holloway et al. [17] and later approved and confirmed by Schamel [18]. The trapped particle structures, observed in the experiments of Risoe-group, have been interpreted in terms of electron hole equilibria [19,20]. The electron hole is a purely nonlinear phenomena and is due to the particle trapping. The electron hole has been found to be related with the slow electron-acoustic mode which is usually absent in plasma. It can exist due to nonlinear distortions of the electron distribution function. Like ion-acoustic solitons an upper limit for the strength of the electron trapping has been found [19]. Effects of trapped electrons, ions, two-temperature ions for the formation of KdV (Korteweg-de Vries) solitons, double layers are investigated by a number of authors [13–15,21]. But up to now, no one has considered the effects of trapped electrons, nonthermal ions and nonadiabatic dust charge variations all together to study the modulational instability and envelope solitary structure of the dust acoustic waves (DAW).

Our paper is organized as follows: in Section 2, the basic equations describing the dust dynamics are presented and the modified NLSE is derived. Section 3 is devoted to study the modulational instability and the structure of the

[a] e-mail: asesh_r@yahoo.com

envelope solitary wave. Lastly, in Section 4, the conclusion is presented.

2 Basic equations and the derivation of NLSE

We consider the propagation of dust acoustic wave in an unmagnetized collisionless plasma consisting of extremely massive and highly negatively charged warm dust grains of equal radii, positively charged nonisothermal ions together with free and trapped electrons. Thus, at equilibrium the overall charge neutrality condition gives

$$\delta_2 = 1 + \delta_1 \tag{1}$$

where $\delta_2 = n_{i0}/Z_{d0}n_{d0}, \delta_1 = n_{e0}/Z_{d0}n_{d0}$ with $n_{\alpha 0}, \alpha = e, i, d$ respectively stand for unperturbed number densities for electron, ion and dust, and Z_{d0} is the number of electrons residing on the dust grain surface. The nonlinear dynamics of the DA waves in such a dusty plasma is governed by

$$\frac{\partial n_d}{\partial t} + \frac{\partial}{\partial x}(n_d u_d) = 0 \tag{2}$$

$$\frac{\partial u_d}{\partial t} + u_d\frac{\partial u_d}{\partial x} + 3\sigma_d n_d\frac{\partial n_d}{\partial x} - Z_d\frac{\partial \phi}{\partial x} = 0 \tag{3}$$

$$\frac{\partial^2 \phi}{\partial x^2} = Z_d n_d + n_e - n_i \tag{4}$$

where n_d and u_d are the dust number density and dust fluid velocity normalized to $Z_{d0}n_{d0}$ and C_d(dust acoustic speed)$= \sqrt{Z_{d0}T_{eff}/m_d}$ with $T_{eff} = Z_{d0}n_{d0}T_iT_e/(n_{i0}T_e + n_{e0}T_i); T_i, T_e$ being the ion and electron temperature and m_d the dust mass; ϕ is the electrostatic potential normalized to T_{eff}/e with e being the elementary charge. Also $\sigma_d = T_d/(Z_{d0}T_{eff})$. Moreover, the space coordinate (x) and time (t) are normalized to the Debye length $\lambda_D = \sqrt{T_{eff}/4\pi Z_{d0}n_{d0}e^2}$ and the inverse of the dust plasma frequency $\omega_{pd} = \sqrt{4\pi Z_{d0}^2 e^2 n_{d0}/m_d}$. The third term proportional to σ_d in equation (3) arises from the pressure gradient force ∇p where we have used the thermodynamic equation of state $p = Cn_d^\gamma$ where C is a constant and γ is the ratio of specific heats and $\gamma = (2 + N)/N$, N being the number of degrees of freedom. For nonisothermal compression we take $N = 1$, so that $\gamma = 3$. The validity of the equation of state requires that heat flow be negligible, i.e., that thermal conductivity be low. Fortunately, most basic phenomena can be described adequately by the crude assumption of equation $p = Cn_d^\gamma$ [6,14,15]. In equation (3) we did not take into account the ion-drag force on the assumption that the electrostatic force dominates over the ion-drag and neutral-drag force. The ion-drag force exerted on a negatively charged dust grains by ion flows ubiquitous in discharge plasmas contributes significantly to the dust transport, formation of equilibrium dust layers and formation of various structures in complex plasmas. In addition to the drag due to the direct collection of ions and to momentum transfer by ions in the electric field near grains, dust grains can also be subject to a drag force due to the effect of coherent waves, such as DAWs that can grow due to the drift of plasma ions relative to charged grains because of an imposed electric field. This force has been extensively studied by a number of authors both theoretically and experimentally [22]. Recently, Yaroshenko et al. [22c] published a paper dealing with the determination of the ion-drag force in a complex plasma. They obtained the said force as a function of a gas pressure (over a pressure range 20–120 Pa). The regime they also investigated where the ion-drag and neutral-drag is much weaker than the electric force. They also pointed out that the particle charge Z_d and ion-drag force (F_i) are in general unknown functions of the neutral gas pressure. The dependencies of Z_d and F_i on p arise due to the variations of the plasma parameters viz., plasma densities, ion-drift velocity, electron temperature, screening length, mean free path etc. with the gas pressure. For the stable particle flow we have

$$F_n = F_E + F_i,$$

where F_n, F_E, F_i respectively stand for neutral-drag, electrostatic and ion-drag forces. However, Yaroshenko et al. have shown that at $p \sim 120$ Pa, for a fixed $F_i/F_E = 0.1$, $F_n/F_E = 0.9$ and for the charge profiles, at $p \sim 20$ Pa, $F_i/F_E = 0.6(0.5)$, $F_n/F_E = 0.4(0.5)$ for small particles (large grains). This means that F_E remains the principal force determining the direction of the particle flow as always observed in the experiment. However, at argon gas pressure ($p \sim 0.2$ Pa) with $T_e = 2$ eV, $T_i = 0.1$ eV, $n_{i0}/n_{e0} = 10$ it can be estimated that $\nu_{dn}/\omega_{pd} \sim 10^{-3}$. But at a higher pressure the same can be treated as a first order quantity, so that it may introduce a damping term in the linear equations. In our plasma model we have neglected the ion-drag force due to ion-dust and dust-ion collisions and the frictional force due to neutral-dust collisions. In a dusty plasma, the ratios of ion-dust and neutral-dust collisions are $\nu_{di}/\nu_{id} \sim m_i n_i/m_d n_d$ and $\nu_{dn}/\nu_{nd} \sim m_n n_n/m_d n_d$. For a typical dusty argon plasma with $m_i/m_d \sim 10^{-20}$–10^{-10}, $m_n/m_d \sim 10^{-14}$–10^{-10}, $n_i/n_d \sim 10^5$, $n_n/n_d \sim 10^8$, $\nu_{di}/\nu_{id} \sim 10^{-15}$–$10^{-5}$ and $\nu_{dn}/\nu_{nd} \sim 10^{-6}$–$10^{-2}$ In our numerical calculations we have considered $m_i/m_d \sim 10^{-16}, m_n/m_d \sim 10^{-14}, n_i/n_d \sim 10^5, n_n/n_d \sim 10^8$ (other parameters as above) for a dusty argon plasma and neglected the collisional effects.

The dust charge dynamics is governed by the following normalized orbital motion limited charge current balance equation

$$\frac{\tau_{ch}}{\tau_d}\left(\frac{\partial Z_d}{\partial t} + u_d\frac{\partial Z_d}{\partial x}\right) = -\frac{\tau_{ch}}{Z_{d0}e}(I_e + I_i). \tag{5}$$

Assume that the streaming velocities of electrons and ions are much smaller than their thermal velocities, the electron and ion currents (I_e, I_i) for spherical grains of equal radii a are given by

$$I_e = -\pi a^2 e\sqrt{\frac{8T_e}{\pi m_e}}n_e \exp(s\sigma_i\Psi) \tag{6}$$

$$I_i = \pi a^2 e\sqrt{\frac{8T_i}{\pi m_i}}n_i(1 - s\Psi). \tag{7}$$

In equation (5) $\tau_d = \omega_{pd}^{-1}$ is the hydrodynamic time scale and τ_{ch} the dust charging time scale given by

$$\tau_{ch}^{-1} = \sqrt{8\pi} a^2 e \delta_2 V_{Ti} s \Psi_0 (1 + \sigma_i (1 - s\Psi_0)) \tag{8}$$

where $\sigma_i = T_i/T_e, V_{Ti} = T_i/m_i$, $s = 1/(\delta_2 + \delta_1 \sigma_i)$, $\Psi = e \Phi_d/T_{eff}, \Phi_d$ being the dust grain surface potential relative to the plasma potential given by

$$\Psi_0 = \ln\left[\alpha\delta(1 - s\Psi_0)\right]/s\sigma_i \tag{9}$$

where $\alpha = \sqrt{\sigma_i/m}, m = m_i/m_e \approx 1844$ and $\delta = n_{i0}/n_{e0}$. The applicability of the charging equation (5) in the case of strong nonlinearity and particle trapping has been discussed extensively in reference [20].

In the dynamical system, some of the electrons are attached to form charged dust grains and some remaining are bounded back and forth in the potential well loosing energy continuously and thereby trapped. Schamel [12a] presented a new method for constructing a smooth distribution for the trapped particles. Thus, in our system the electron number density in normalized form which is obtained by taking first moment of Schamel's distribution function as

$$n_e(\phi) = \frac{n_{e0}}{n_{d0} Z_{d0}} \Bigg[\exp(\Gamma)\mathrm{erfc}(\sqrt{\Gamma}) + \frac{1}{\sqrt{|\beta_h|}} \begin{cases} \exp(\Gamma\beta_h)\mathrm{erf}(\sqrt{\Gamma\beta_h}) & \beta_h \geq 0 \\ \frac{2}{\sqrt{\pi}} \exp(\Gamma\beta_h) \int_0^{\sqrt{-\Gamma\beta_h}} \exp(t^2) dt & \beta_h < 0 \end{cases} \Bigg] \tag{10}$$

where $\Gamma = e\phi/T_e, \beta_h = T_e/T_t$ with T_t the trapped electron temperature. The electron density includes four types of distributions namely, (i) the Maxwellian where $\beta_h \to 1$, (ii) the flat topped one where $\beta_h = 0$, (iii) a hole in the trapped region representing a vortex type distribution where $\beta_h < 0$ and (iv) the fourth type where $0 < \beta_h < 1$. In our plasma model we assume $0 < \beta_h < 1$. Now expanding equation (10) for small arguments by Taylor series we write the expression for n_e [14] as

$$n_e \approx \delta_1 \left[1 + (s\sigma_i\phi) + (s\sigma_i\phi)^2 - G(s\sigma_i\phi)\right] \tag{11}$$

where

$$G(x) = \sum_{k=1}^{2} \left[2^{k+1} b_k x^{(2k+1)/2} / \prod(2k+1)\right] \tag{12}$$

with $b_k = (1 - \beta_h^k)/\sqrt{\pi}$. On the other hand, the ion density distribution is assumed to describe by the following [23,24]

$$n_i = \delta_2 \left(1 + \beta\phi + \beta\phi^2\right) \exp(-s\phi)$$

i.e.,

$$n_i \approx \delta_2 \left[1 + (\beta - s)\phi + \left[\beta(1 - s) + \frac{1}{2}s^2\right]\phi^2\right] \tag{13}$$

for small arguments. Here $\beta = 4\eta/(1 + 3\eta)$ with η being a parameter determining the number of nonthermal ions. Mendonza-Briceno et al. [23] used such type of distribution for nonthermal ions in a dusty plasma and they found that the nonthermality of ions can significantly change the nature of the Dust-acoustic waves. It is to be mentioned that another way of deviation from the usual Boltzmann distribution of ions would be to take into account the effects of trapped ions which would lead to an expression like equation (10) for the ion density.

In order to investigate the amplitude modulation of DAW in our plasma we employ the standard reductive perturbation technique to obtain NLSE with the stretching: $\xi = \sqrt{\epsilon}(x - v_g t), \tau = \epsilon t$ where ϵ is a small parameter which usually reflects directly the strength of the wave amplitude and v_g is the group velocity of the wave. The dynamical variables are expanded as:

$$n_d = 1 + \sum_{n=1}^{\infty} \epsilon^{n/2} \sum_{l=-\infty}^{\infty} n_l^{(n)}(\xi, \tau) \exp(ikx - i\omega t) l \tag{14}$$

$$u_d = \sum_{n=1}^{\infty} \epsilon^{n/2} \sum_{l=-\infty}^{\infty} u_l^{(n)}(\xi, \tau) \exp(ikx - i\omega t) l \tag{15}$$

$$\phi = \sum_{n=1}^{\infty} \epsilon^{n/2} \sum_{l=-\infty}^{\infty} \phi_l^{(n)}(\xi, \tau) \exp(ikx - i\omega t) l \tag{16}$$

$$Z_d = 1 + \sum_{n=1}^{\infty} \epsilon^{n/2} \sum_{l=-\infty}^{\infty} Z_l^{(n)}(\xi, \tau) \exp(ikx - i\omega t) l \tag{17}$$

where $n_l^{(n)}, u_l^{(n)}$ etc. satisfy the reality condition $A_l^{(n)} = A_l^{(n)*}$ and the asterisk denotes the complex conjugate. Typically, the dust charging time scale is of the order of 10^{-6}–10^{-5} s, so that $\tau_{ch} \ll \tau_d$ and we can assume that $\tau_{ch}/\tau_d = \mu\epsilon$ where μ is a finite quantity of the order of unity. Now substituting the expressions (11), (13–17) into equations (2–5) and collecting the terms in different powers of ϵ we obtain for $n = 1, l = 1$ the first order quantities:

$$n_1^{(1)} = -\frac{k^2}{\omega^2 - 3\sigma_d k^2} \phi_1^{(1)} \tag{18}$$

$$u_1^{(1)} = -\frac{\omega k}{\omega^2 - 3\sigma_d k^2} \phi_1^{(1)} \tag{19}$$

$$Z_1^{(1)} = \gamma_1 \phi_1^{(1)}. \tag{20}$$

The dispersion relation is then obtained for the DAW from equations (18–20) as:

$$\omega^2 = 3\sigma_d k^2 + \frac{k^2}{1 - \beta\delta_2 + \gamma_1 + k^2} \tag{21}$$

where the variable γ_1 for the dust charge fluctuation effect is given by

$$\gamma_1 = \frac{(1 + \sigma_i - \beta/s)(1 - s\Psi_0)}{\Psi_0(1 + \sigma_i(1 - s\Psi_0))}. \tag{22}$$

The second order ($n = 2$) reduced equations with $l = 1$ give

$$n_1^{(2)} = 2ki\frac{\partial\phi_1^{(1)}}{\partial\xi} - \frac{k^2}{\omega^2 - 3\sigma_d k^2}\phi_1^{(2)} \tag{23}$$

$$u_1^{(2)} = \frac{i}{\omega}\left(\omega^2 + 3\sigma_d k^2\right)\frac{\partial\phi_1^{(1)}}{\partial\xi} - \frac{\omega k}{\omega^2 - 3\sigma_d k^2}\phi_1^{(2)} \tag{24}$$

$$Z_1^{(2)} = \gamma_1\phi_1^{(2)} \tag{25}$$

together with the compatibility condition:

$$v_g \equiv \frac{\partial\omega}{\partial k} = \frac{\omega^2 - (\omega^2 - 3\sigma_d k^2)^2}{\omega k}. \tag{26}$$

The second harmonic modes ($n = 2, l = 2$) arising from the nonlinear self-interaction of the carrier wave are obtained in terms of $[\phi_1^{(1)}]^2$ as:

$$\phi_2^{(2)} = A\left[\phi_1^{(1)}\right]^2 \tag{27}$$

$$n_2^{(2)} = B\left[\phi_1^{(1)}\right]^2 \tag{28}$$

$$u_2^{(2)} = C\left[\phi_1^{(1)}\right]^2 \tag{29}$$

$$Z_2^{(2)} = D\left[\phi_1^{(1)}\right]^2 \tag{30}$$

where the coefficients A, B, C, D are given as follows:

$$A = \left[\left\{\frac{1}{2}\left(-G + \sqrt{G^2 + 4H^3}\right)\right\}^{1/3} + \left\{\frac{1}{2}\left(-G - \sqrt{G^2 + 4H^3}\right)\right\}^{1/3} + \frac{2}{3}b_1\delta_1(s\sigma_i)^{3/2}\right]^2 /E^2 \tag{31}$$

$$G = \frac{1}{6}E(s\sigma_i)^{3/2}\left\{(b_2\delta_1 s\sigma_i - 3b_1\gamma_1)E + 4b_1\delta_1 F\right\} - \frac{16}{27}\left\{b_1\delta_1(s\sigma_i)^{3/2}\right\}^3 \tag{32}$$

$$H = \frac{1}{9}\left[3EF - 4b_1^2\delta_1^2(s\sigma_i)^3\right] \tag{33}$$

$$E = \frac{1}{2}\frac{k^2}{(\omega^2 - 3\sigma_d k^2)^3} + \delta_1 s\sigma_i - \delta_2(\beta - s) + 4k^2 - \gamma_1 \tag{34}$$

$$E_1 = 3k^2\left(\omega^2 + \sigma_d k^2\right) - \gamma_1(\omega^2 - 3\sigma_d k^2)^2 \tag{35}$$

$$E_2 = \frac{s}{2}\left(1 - \frac{\sigma_i^2}{\alpha\delta}(1+\gamma_1\Psi_0)^2\right) - \beta(1 - 1/s) - \gamma_1\Psi_0(\beta - s) \tag{36}$$

$$F = \frac{1}{2}\delta_1(s\sigma_i)^2 - \delta_2\left\{\beta(1-s) + s^2/2\right\} - \frac{k^2 E_1}{\omega^2 - 3\sigma_d k^2}\left[\gamma_1 + \frac{1}{2(\omega^2 - 3\sigma_d k^2)^2}\right] - \frac{E_2}{\Psi_0\left(1 + \sigma_i(1 - s\Psi_0)\right)} \tag{37}$$

$$B = \frac{(E_1 - A)k^2}{2(\omega^2 - 3\sigma_d k^2)^3} \tag{38}$$

$$C = \frac{\omega k}{2(\omega^2 - 3\sigma_d k^2)^3}\left\{k^2(\omega^2 + 9\sigma_d k^2) - \gamma_1(\omega^2 - 3\sigma_d k^2)^2 - A\right\} \tag{39}$$

$$D = \frac{E_2}{\Psi_0\left(1 + \sigma_i(1 - s\Psi_0)\right)} + \gamma_1\left(A + \frac{1}{2}b_1(s\sigma_i)^{3/2}/\sqrt{A}\right). \tag{40}$$

Similarly, the zeroth harmonic modes which appear due to the self-interaction of the modulated carrier wave are obtained for $l = 0, n = 2$ as:

$$\phi_0^{(2)} = A_0|\phi_1^{(1)}|^2 \tag{41}$$

$$n_0^{(2)} = B_0|\phi_1^{(1)}|^2 \tag{42}$$

$$u_0^{(2)} = C_0|\phi_1^{(1)}|^2 \tag{43}$$

$$Z_0^{(2)} = D_0|\phi_1^{(1)}|^2 \tag{44}$$

where the coefficients A_0, B_0, C_0, D_0 are

$$A_0 = [4E_2 - \Psi_0(1 + \sigma_i(1 - s\Psi_0))A_1]/A_2 \tag{45}$$

$$A_1 = \frac{2k^2}{\omega^2 - 3\sigma_d k^2}\left\{\gamma_1 + \frac{\omega k v_g}{(3\sigma_d - v_g^2)(\omega^2 - 3\sigma_d k^2)}\right\} - \delta_1(s\sigma_i)^2 + 2\delta_2\left[\beta(1-s) + s^2/2\right] \tag{46}$$

$$A_2 = (1 - s\Psi_0)(1 + \sigma_i - \beta/s) - \Psi_0\left[1 + \sigma_i(1 - s\Psi_0)\right] \times \left\{s\sigma_i\delta_1 - (\beta - s)\delta_2 + (3\sigma_d - v_g^2)^{-1}\right\} \tag{47}$$

$$B_0 = \frac{1}{3\sigma_d - v_g^2}\left[A_0 - \frac{2\omega v_g k^3}{(\omega^2 - 3\sigma_d k^2)^2}\right] \tag{48}$$

$$C_0 = \frac{1}{3\sigma_d - v_g^2}\left[A_0 v_g - \frac{6\omega\sigma_d k^3}{(\omega^2 - 3\sigma_d k^2)^2}\right] \tag{49}$$

$$D_0 = [(1 - s\Psi_0)(1 + \sigma_i - \beta/s)A_1 - 4E_2\left\{s\sigma_i\delta_1 - (\beta - s)\delta_2 + (3\sigma_d - v_g^2)^{-1}\right\}]/A_2. \tag{50}$$

Finally, substitutions of all the above derived expressions into the $l = 1$ component of the third order part ($n = 3$) of the reduced equations lead to the following modified NLSE for the DA waves with trapped electrons and nonthermal ions

$$i\frac{\partial\phi}{\partial\tau} + P\frac{\partial^2\phi}{\partial\xi^2} + Q|\phi|^2\phi = iR\phi \tag{51}$$

where $\phi \equiv \phi_1^{(1)}$ and the coefficients P, Q, R are given by

$$P = -\frac{3(\omega^2 - 3\sigma_d k^2)}{2\omega^2 k}\left[-4\sigma_d k\omega + v_g(\omega^2 + \sigma_d k^2)\right] \tag{52}$$

$$Q = -\frac{(\omega^2 - 3\sigma_d k^2)^2}{2\omega k^2}\left[\frac{\lambda_4 - s\Psi_0\lambda_3(1 + \sigma_i(1 - s\Psi_0))}{s\Psi_0(1 + \sigma_i(1 - s\Psi_0))} + \frac{\omega\lambda_1 + k\lambda_2}{\omega^2 - 3\sigma_d k^2}\right] \tag{53}$$

$$R = (\omega^2 - 3\sigma_d k^2)^2 Z_{d0} e\gamma_1\mu/2k^2 \tag{54}$$

$$\lambda_1 = \frac{k^3}{\omega^2 - 3\sigma_d k^2}\left\{C + C_0 + \frac{\omega}{k}(B + B_0)\right\} \tag{55}$$

$$\lambda_2 = \frac{k^2}{\omega^2 - 3\sigma_d k^2}\left\{\omega(C + C_0) + 3\sigma_d k(B + C_0)\right\} + k(2A\gamma_1 + D_0 - D) \tag{56}$$

$$\lambda_3 = (A + A_0)\left[\delta_1(s\sigma_i)^2 - 2\delta_2\left\{\beta(1-s) + s^2/2\right\}\right] + \frac{1}{2}\left[\delta_1(s\sigma_i)^3 + s\delta_2\left\{3\beta(2-s) + s^2\right\}\right] + \frac{(D + D_0)k^2}{\omega^2 - 3\sigma_d k^2} - (B + B_0)\gamma_1 \tag{57}$$

$$\lambda_4 = -\frac{(s\sigma_i)^2}{\alpha\delta}(1 + \Psi_0\gamma_1)\Big[A + A_0 + \psi_0(D + D_0) + \frac{1}{2}s\sigma_i(1 + \Psi_0\gamma_1)^2\Big] + (A + A_0)\left[2\left\{\beta(1-s) + s^2/2\right\} - s(\beta - s)\Psi_0\gamma_1\right] - s\Psi_0(\beta - s)(D + D_0). \tag{58}$$

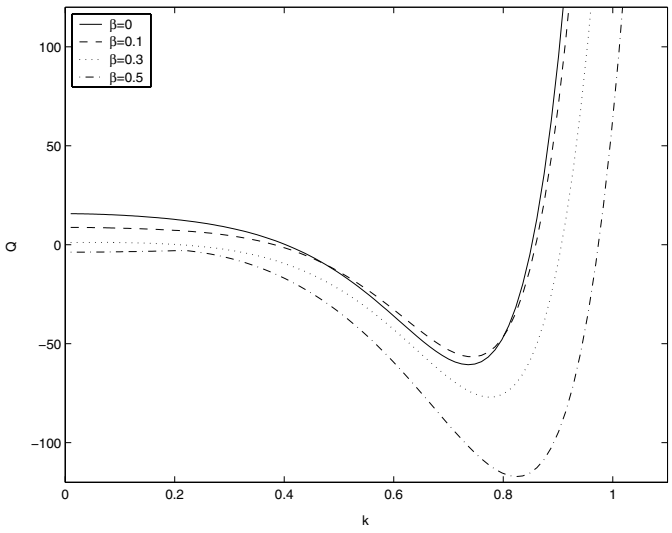

Fig. 1. The variation of Q with respect to k for different values of $\beta = 0, 0.1, 0.3, 0.5$ and for fixed $\delta = 70, \sigma_i = 0.5, \beta_h = 0.4$.

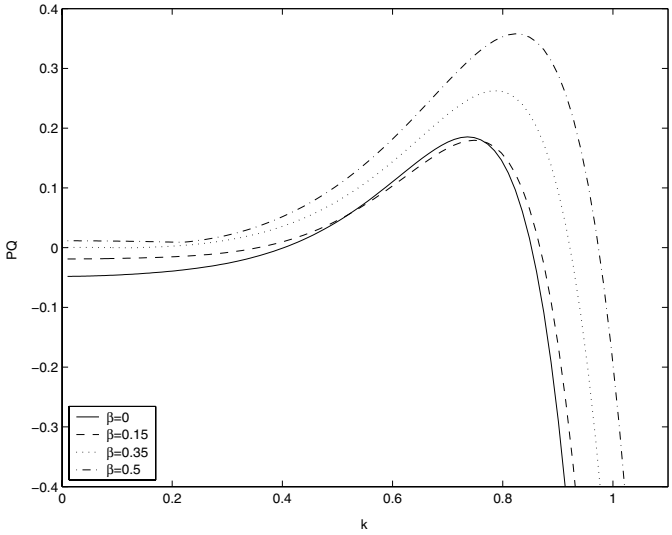

Fig. 2. The plot of PQ vs. k for different values of $\beta = 0$, 0.15, 0.35, 0.5 and for fixed $\delta = 70, \sigma_i = 0.5, \beta_h = 0.4$ showing the stability and instability regions.

We find in equation (51) that the coefficient of the dispersive term (P) remains unchanged as in reference [6], while that of the nonlinear term (Q) gets modified due to the presence of both the trapped electrons and nonisothermal ions. The additional term $iR\phi$ which represents the nonadiabiticity of dust charge variations is modified only by the nonthermal ions (as compared with the term $-i\Gamma\phi$ in Ref. [6]). In absence of trapped electrons and nonthermal ions, i.e., for $b_k = 0, k = 1, 2; \beta = 0$ we can recover the same NLSE as in reference [6]. Hence, it follows that the propagation characteristics and the modulational instability of the DA waves in our dusty plasma system will be modified somewhat.

3 Modulational instability and the envelope soliton

A standard modulational instability analysis [3,6] of the DAW shows that the wave becomes modulationally unstable when $PQ > 0$ in the wave number region $K^2 < K_c^2(\tau)$ with $K_c^2 = (2Q/P)|\phi_0|^2 \exp(2R\tau)$. The instability growth rate is obtained as

$$\Im\Omega(\tau) = PK^2\sqrt{\frac{K_c^2}{K^2} - 1} \tag{59}$$

where Ω represents the modulational frequency. The maximum growth rate at $K = K_c/\sqrt{2}$ is $Q|\phi_0|^2 \exp(2R\tau)$. Which shows that the maximum instability growth rate is proportional to the nonlinearity Q and the amplitude of the pump carrier wave ϕ_0, but inversely proportional to the nonadiabaticity of the dust charge variation R. We recall that P is unaffected by the new parameters β, β_h; Q is affected by both of them and R is only by β. Figure 1 shows the variation of Q with respect to k for different values of $\beta = 0, 0.1, 0.3, 0.5$ and for fixed $\delta = 70, \sigma_i = 0.5, \beta_h = 0.4$. We find that for $k < 0.23$, $Q > 0$ at $\beta = 0, 0.1, 0.3$ whereas $Q < 0$ at $\beta = 0.5$, i.e., as β increases Q tends to become negative at short range of k and the range of values of k increases as $\beta(< 1)$ increases. Figure 2 shows that the range of k for which the wave becomes unstable ($PQ > 0$) increases for increasing values of β. It is also clear that for isothermal ions $\beta = 0$ the wave packet becomes unstable in the long-wave length region, whereas in case of nothermal ions a critical value of β must exist for the instability in the long-wave length run. Figures 3 and 4 show the variation of Q with k for fixed $\delta = 80, \sigma_i = 0.3$ and for different values of β and β_h. From Figure 4 it is clear that the nonthermality of electrons and

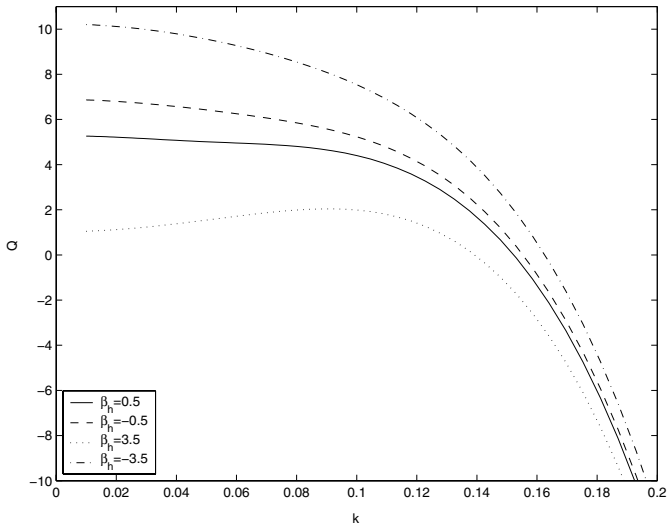

Fig. 3. The variation of Q with respect to k for different values of $\beta_h = 0.5, -0.5, 3.5, -3.5$ and for fixed $\delta = 80, \sigma_i = 0.3$, $\beta = 0.3$.

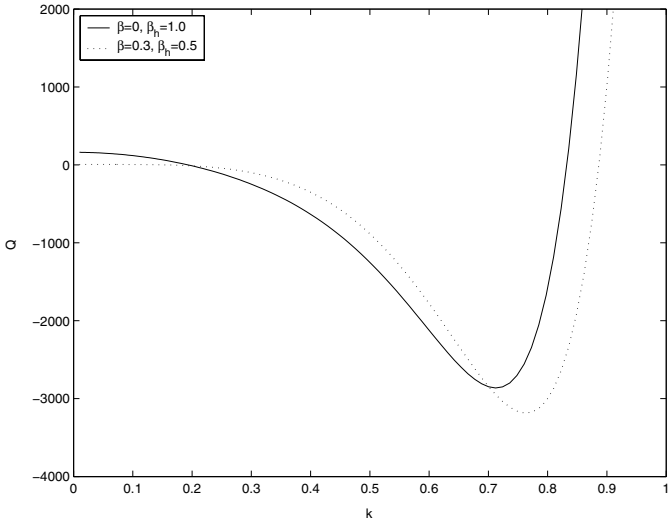

Fig. 4. The thermal and nonthermal effects of electrons and ions on the variations of Q with respect to k for $\beta = 0, \beta_h = 1$ and for $\beta = 0.3, \beta_h = 0.5$ where $\delta = 80, \sigma_i = 0.3$.

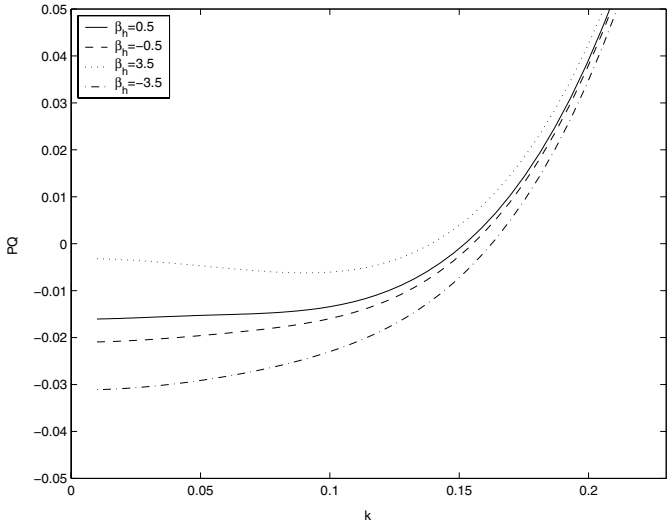

Fig. 5. The stability and instability regions: the plot of PQ vs. k for different values of $\beta_h = 0.5, -0.5, 3.5, -3.5$ and other parameter values as in Figure 3.

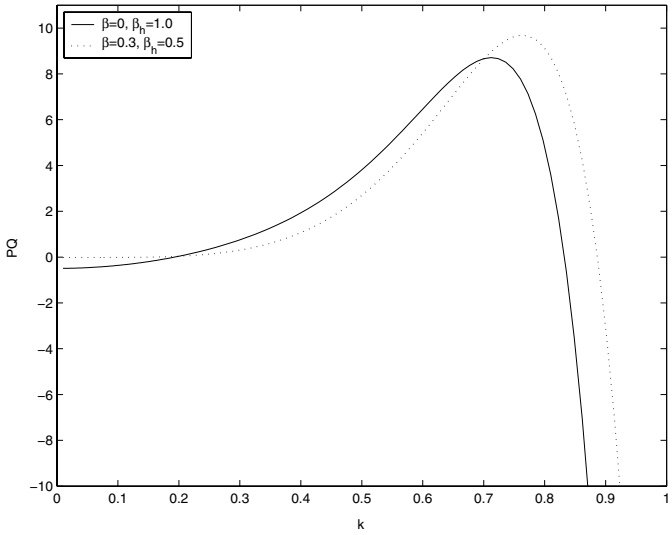

Fig. 6. The thermal and nonthermal effects on the stability/ instability regions. PQ vs. k diagram; parameter values are as in Figure 5.

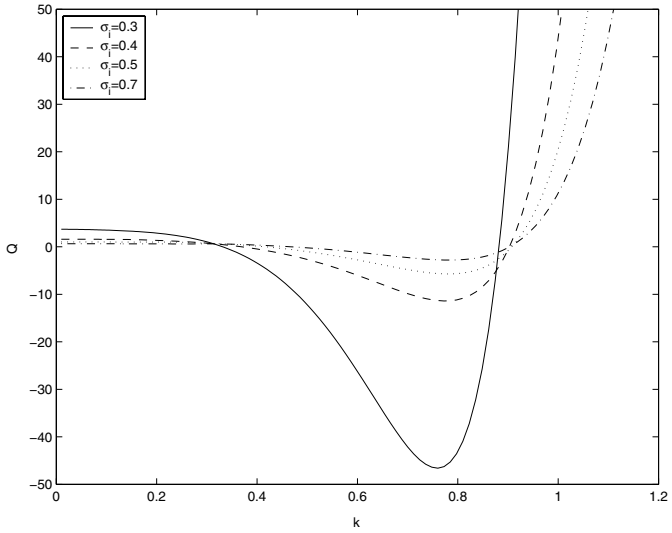

Fig. 7. The variation of Q with respect to k for different values of $\sigma_i = 0.3, 0.4, 0.5, 0.7$ and for fixed $\delta = 90, \beta = 0.2, \beta_h = 0.5$.

ions is to make Q negative in the short range $k < 0.2$ and positive in the comparatively long k-range ($k > 0.87$). Figures 5 and 6 show the stability and instability regions for various β and β_h values and for fixed $\delta = 80, \sigma_i = 0.3$. We find that the nothermal electrons and ions play crucial role to cause modulational instability. In Figures 7 and 8, the variations of Q, PQ are shown for different σ_i-values and for fixed $\delta = 90, \beta = 0.2, \beta_h = 0.5$. Form Figure 8, it is clear that the instability region in a fixed k-domain is greater at $\sigma_i = 0.3$. Figure 9 shows that as β increases the magnitude of the nonadiabaticity R decreases in the short-wave length run. It is to be mentioned that an exact analytic solution of the NLSE (51) is not possible, except for some cases where an inverse scattering transformation method [25] can be applied for this purpose. For example, when $PQ > 0$ we have the perturbation solution [6] for small R

$$\phi = 2i\phi_0 \exp(2R\tau)\mathrm{sech}\left(2\phi_0 \exp(2R\tau)\sqrt{\frac{Q}{2P}}(\xi + \sqrt{2PQ}c\tau)\right) \times \exp\left[-i\sqrt{\frac{Q}{2P}}\left(c\xi + c^2\sqrt{\frac{PQ}{2}}\tau + \frac{\phi_0^2}{R}\sqrt{\frac{PQ}{2}}(\exp(4R\tau) - 1)\right)\right] \quad (60)$$

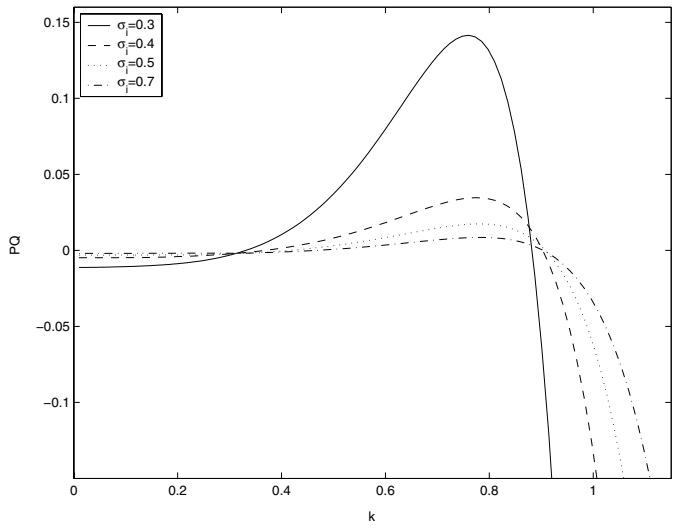

Fig. 8. The same as in Figure 5, but for different $\sigma_i = 0.3$, 0.4, 0.5, 0.7. The other parameter values are the same as for Figure 7.

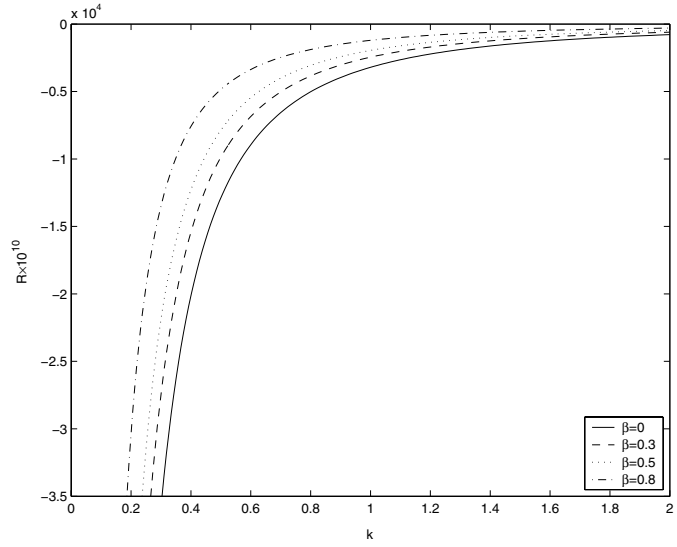

Fig. 9. The variation of R with k for $\beta = 0, 0.3, 0.5, 0.8$ where $\delta = 50, \sigma_i = 0.2$.

where c is a constant. It is clear from equation (60) that as time elapses the amplitude of the envelope solitary wave tends to decrease exponentially. The nonadiabaticity of dust charge variations is to cause a damping effect, which can be minimized at higher value of $\beta(< 1)$ (Fig. 9) in the long-wave length region. Another form of envelope soliton ($PQ > 0$) can be obtained for $R = 0$ [9] as

$$\phi = \phi_0 \mathrm{sech}\left(\sqrt{\left|\frac{Q}{2P}\right|}\phi_0\xi\right)\exp(i\sigma(\xi,\tau)) \qquad (61)$$

where σ is a real constant. On the other hand, for $PQ < 0$ the wave can propagate in the form of an envelope hole

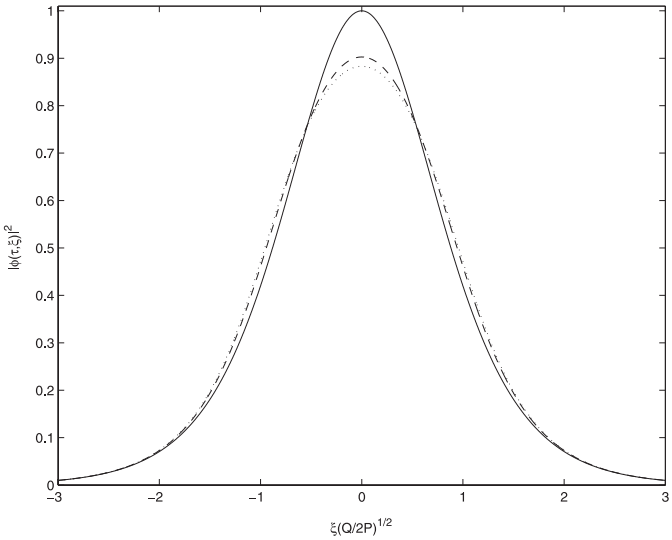

Fig. 10. The initial (solid line) and final pulse shapes for isothermally distributed electrons and ions ($\beta = 0, \beta_h = 1$). The dotted and dashed line correspond to $P = -3.04 \times 10^{-3}$, $Q = -10.0, R = -0.25 \times 10^{-5}$ at $k = 0.495$ and $P = -3.03 \times 10^{-3}, Q = -7.98, R = -0.84 \times 10^{-6}$ at $k = 0.848$ respectively. Other parameter values are $\delta = 90, \sigma_i = 0.3$.

(dark soliton) or envelope shock [9]. In order to solve our problem, it is therefore necessary a numerical approach for an understanding of the nonlinearities. A large number of numerical methods can be used for this purpose (please refer to Refs. [49–64] in chapter two of "Nonlinear Fiber Optics", third edn., by G.P. Agrawal). However, one best is the split-step Fourier method [26]. To this end we recast the NLSE as

$$i\frac{\partial\phi}{\partial\tau} + \frac{1}{2}\frac{\partial^2\phi}{\partial\xi^2} + |\phi|^2\phi = i\frac{R}{Q}\phi \qquad (62)$$

where we have made the normalizations: $\tau \to \tau Q, \xi \to \xi\sqrt{(Q/2P)}$. The initial ($\mathrm{sech}(\xi\sqrt{(Q/2P)})$) and final pulse shapes, and the initial and final pulse spectra (Fourier transformed) in case of thermal and nonthermal electrons and ions are shown in Figures 10, 11 and 12, 13. For Figures 10 and 11 we have taken $\delta = 90, \sigma_i = 0.3, \beta = 0, \beta_h = 1$. We find from Figure 10 that the soliton pulse height for $P \approx -3.03 \times 10^{-3}, Q \approx -7.98$ at $k = 0.848$ is greater than that for $P \approx -3.04 \times 10^{-3}, Q \approx -10.0$ at $k = 0.495$. On the other hand, Figure 12 where we have taken $\delta = 90, \sigma_i = 0.3, \beta = 0.3, \beta_h = 0.5$ shows that the pulse height for $P \approx -3.04 \times 10^{-3}, Q \approx -0.85$ at $k = 0.244$ is greater than those for $P \approx -3.04 \times 10^{-3}, Q \approx -10.1$ at $k = 0.429$ and for $P \approx -3.03 \times 10^{-3}, Q \approx -4.2$ at $k = 0.914$. That is, the nonthermality of electrons and ions changes qualitatively the soliton shapes quite distinct from the isothermal ones.

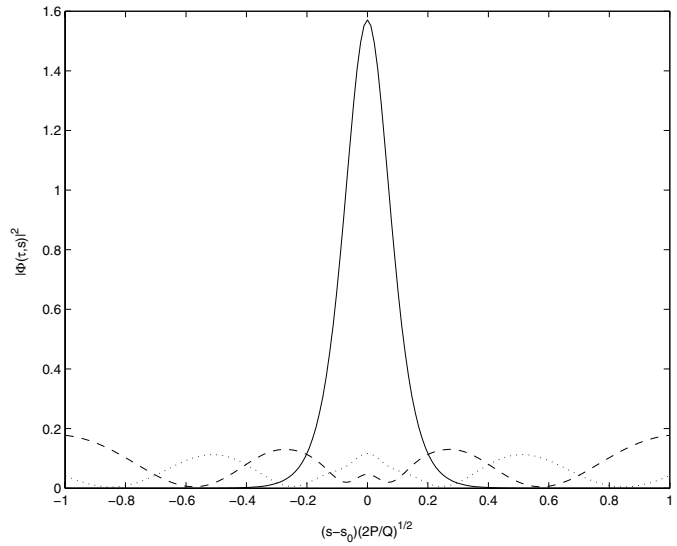

Fig. 11. The initial (solid line) and final pulse spectra for isothermally distributed electrons and ions ($\beta = 0, \beta_h = 1$). The dotted and dashed line correspond to the same as in Figure 10.

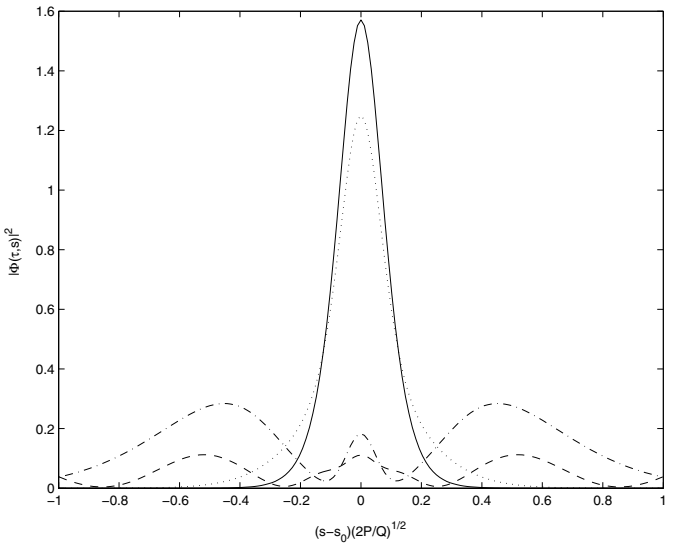

Fig. 13. The initial and final pulse spectra for nonthermally distributed electrons and ions ($\beta = 0.3, \beta_h = 0.5$). The dotted, dashed and dash-dotted line correspond to the same as in Figure 12.

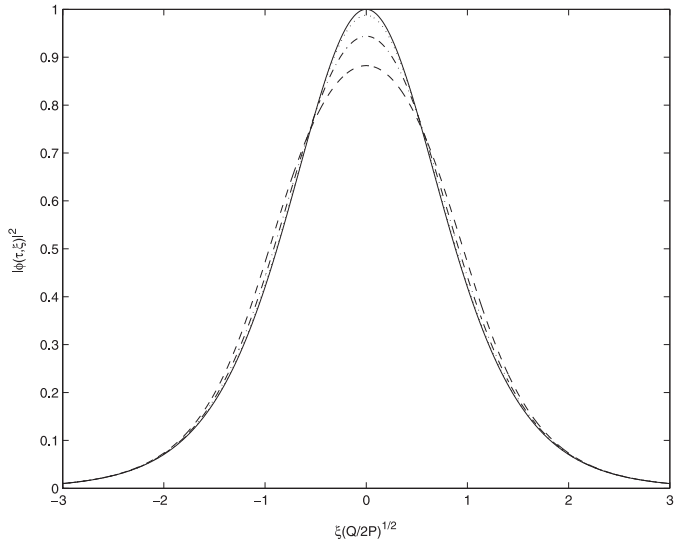

Fig. 12. The initial (solid line) and final pulse shapes for nonthermally distributed electrons and ions ($\beta = 0.3, \beta_h = 0.5$). The dotted, dashed and dash-dotted line correspond to $P = -3.04 \times 10^{-3}, Q = -0.85, R = -0.78 \times 10^{-5}$ at $k = 0.245$, $P = -3.04 \times 10^{-3}, Q = -10.1, R = -0.25 \times 10^{-5}$ at $k = 0.429$ and $P = -3.03 \times 10^{-3}, Q = -4.2, R = -0.56 \times 10^{-6}$ at $k = 0.914$ respectively. Other parameter values are $\delta = 90, \sigma_i = 0.3$.

4 Conclusions

In our above analysis we have tried to modify the previous work [6] by incorporating the effects of trapped electrons and nonisothermal ions. A modified NLSE describing the slow modulation of DA waves in an unmagnetized warm dusty plasma with nonadiabaticity of dust charge variations, trapped electrons and nonthermally distributed ions is derived by the standard reductive perturbation technique and is solved numerically by the split-step Fourier method. The effects of trapped electrons and nonthermal ions on the modulational instability and soliton structures are discussed. It is found that by these effects the instability domains for the wave packet are significantly changed, and the soliton pulse width and amplitude are somewhat modified. It is to be mentioned that the inclusion of trapping of ions caused by the ion-neutral collisions will be an another important investigation in this nonlinear analysis, but beyond the scope of the present work.

The authors wish to thank the referees for their valuable comments which improved the paper in its present form.

References

1. K. Schimizee, Y.H. Ichikawa, J. Phys. Soc. Jpn **33**, 789 (1972)
2. K. Kakutani, N. Sugimoto, Phys. Fluids **17**, 1617 (1974)
3. M.R. Amin, G.E. Morphil, P.K. Shukla, Phys. Rev. E **58**, 6517 (1998)
4. M. Kaka, A. Hasegawa, Phys. Fluids **19**, 1976 (1967)
5. T. Yashvir, N. Bhatnagar, S.R. Sharma, Phys. Fluids **29**, 128 (1986)
6. Ju-Kui Xue, Phys. Lett. A **320**, 226 (2003)
7. Xue Jukui, Chaos, Solitons & Fractals **18**, 849 (2003)
8. Wen-shan Duan et al., Chaos, Solitons & Fractals **16**, 767 (2003)
9. Wen-shan Duan, J. Parkes, Lei Jhang, Phys. Plasmas **11**, 3762 (2004)
10. A.P. Misra, A. Roy Chowdhury, Fizika A (Zagreb) **11**, 163 (2002)

11. J.P. Lynov et al., Phys. Lett. **80**, 23 (1980)
12. H. Schamel, J. Plasma Phys. **9**, 377 (1973) and the references cited therein; Y.-N. Nejoh, J. Plasma Phys. **56**, 57 (1996); A.A. Mamun, R.A. Cairns, P.K. Shukla, Phys. Plasmas **3**, 2610 (1996)
13. Y.-N. Nejoh, Phys. Plasmas **4**, 2813 (1997)
14. S.K. El-Labany, W.F. El-Taibany, Phys. Plasmas **10**, 4685 (2003)
15. S.K. El-Labany et al., Phys. Plasmas **11**, 926 (2004)
16. D. Bohm, E.P. Gross, Phys. Rev. **75**, 1851 (1949)
17. J.P. Holloway, J.J. Dorning, Phys. Rev. A **44**, 3856 (1991)
18. H. Schamel, Phys. Rev. Lett. **79**, 2811 (1997); H. Schamel, Phys. Plasmas **7**, 4831 (2000)
19. H. Schamel, Phys. Scr. **20**, 336 (1979)
20. H. Schamel, Phys. Rep. **140**, 161 (1986)
21. M.S. Barnes et al., Phys. Rev. Lett. **68**, 313 (1992); A.P. Misra, A. Roy Chowdhury, Eur. Phys. J. D **37**, 105 (2006)
22. S.A. Khrapak et al., Phys. Rev. E **66**, 046414 (2002); S.A. Khrapak et al., Phys. Rev. Lett. **90**, 225002 (2003); V. Yaroshenko et al., Phys. Plasmas **12**, 093503 (2005); A.V. Ivlev et al., Plasma Phys. Control. Fusion **46**, B267 (2004)
23. C.A. Mendoza-Briceno, S.M. Russel, A.A. Mamun, Planet. Space Sc. **48**, 599 (2000)
24. A.A. Mamun, N.N. Alam, Phys. Scr. **57**, 535 (1998)
25. Y.S. Kivshar, B.A. Malomed, Rev. Mod. Phys. **61**, 763 (1989)
26. G.P. Agrawal, *Nonlinear Fiber Optics*, 2nd edn. (Academic Press, 1995)